221 (2023) 211404

Contents lists available at ScienceDirect

Geoenergy Science and Engineering

journal homepage: www.sciencedirect.com/journal/geoenergy-science-and-engineering

Formation uplift analysis during geological CO_2-Storage using the Gaussian pressure transient method: Krechba (Algeria) validation and South Korean case studies

Sungjun Jun [a], Youngsoo Song [a], Jihoon Wang [a,*], Ruud Weijermars [b]

[a] Department of Earth Resources and Environmental Engineering, Hanyang University, Seoul, 04763, South Korea
[b] Department of Petroleum Engineering & Center for Integrative Petroleum Research (CIPR), College of Petroleum Engineering and Geosciences (CPG), King Fahd University of Petroleum & Minerals, KFUPM, Dhahran, 31261, Saudi Arabia

ARTICLE INFO

Keywords:
Carbon storage
Uplift
Gaussian pressure transient
Krechba gas field
Pohang basin
Donghae gas reservoir

ABSTRACT

The Paris Climate Agreement of 2015, along with the commitments in the South Korean *2050 Carbon-Neutral* Scenario, highlights the importance of carbon capture and storage (CCS) to counter advancing global warming. During CCS, carbon-dioxide enriched fluid is injected into a geological formation, which causes pore pressure increases. The CCS must occur safe and stable, which requires geomechanical modeling to analyze the effects of formation uplift and subsidence. In this study, surface uplift and subsidence were predicted with a recently developed Gaussian pressure transient (GPT) method, in advance of the anticipated CO_2-injection schemes to ensure a secure storage process. The GPT-results were first validated against field observations obtained from the In Salah CCS-site (Algeria). Next, the GPT-method was applied to two potential CCS target locations in South Korea: (1) the Pohang basin, and (2) the Donghae gas reservoir. Maximum uplifts of 25.42 and 32.55 mm, respectively, were estimated for each location. In addition, the effect of installing a relief well to mitigate the uplift was studied. Subsidence was estimated around the relief well due to production. The presence of the relief well aided the mitigation of both uplift and subsidence. Our study shows that preliminary analysis of uplift and subsidence of potential CCS-sites is possible with the GPT-method. In addition, it was shown that installing (one or more) relief well(s) for the purpose of mitigating the severe uplift caused by injection is feasible.

1. Introduction

According to the *2050 Carbon-Neutral* Scenario (Kim et al., 2022) set by the collaborative committees of the South Korean government in 2021, at least 55.1 to 84.6 million tonnes of CO_2-equivalent have to be either stored underground by carbon capture and storage (CCS) or utilized with carbon capture utilization and storage (CCUS) technology by 2050. CCS and CCUS are perceived as the two most viable technologies of sequestrating the CO_2 into underground formations, which contribute to diminishing the greenhouse gas proportion in the atmosphere to mitigate global warming. Therefore, the global efforts to meet the Paris Climate Agreement are led by both public and private sectors. In order to achieve the desired injection and storage schedule set by the South Korean government in support of the Paris Agreement, assessing the secure injection of CO_2 into underground formations is as crucial as meeting the required storage capacity targets.

To ensure the secure injection of CO_2, detailed studies must precede the successful sequestration and permanent storage of the injected fluid. Such studies critically require a geomechanical analysis of the stress regime changes, fracture mechanism, and discontinuity integrity (Kresse and Weng, 2018; Wu and Olson, 2015; Cao and Sharma, 2022a, 2022b). During CO_2-injection into a geological structure, geomechanical response will occur due to the unavoidable pore pressure buildup. If not managed properly, the pressure may exceed a critical limit leading to brittle failure, which may lead to potential leakage of injection fluid (Roberts et al., 2018), accompanied by caprock deflection (Li et al., 2015), fault reactivation (Cappa and Rutqvist, 2011), unintended hydraulic fracturing (Appriou, 2019), unexpected seismic activity (Nicol et al., 2011; Zoback and Gorelick, 2012), and formation deformation (Teatini et al., 2011).

The formation deformation initially may seem less severe to the general public because it accumulates slowly over a certain period with

* Corresponding author.
E-mail address: jihoonwang@hanyang.ac.kr (J. Wang).

https://doi.org/10.1016/j.geoen.2022.211404
Received 7 June 2022; Received in revised form 8 December 2022; Accepted 26 December 2022
Available online 29 December 2022

a small amount of uplift or subsidence that may not be noted by unaided human sense (Teatini et al., 2011). However, when the deformation occurs and increases, the effect can be critical (Ferronato et al., 2010; Widdicombe et al., 2013; Wei et al., 2011). Severe deformation near well locations may damage the surface or seabed facilities of fluid extraction and production projects by compromising the alignment of blowout preventers (BOP), tubing hangers, casing hangers, cellars, master valves, etc. (Donovan et al., 2002; Hoffmann et al., 2001) In addition, uplift may be accompanied by unintended hydraulic fracturing of the underground channels (Sun, 1969).

A well-known field study observed the formation uplift in the Krechba gas field at In Salah, Algeria. Approximately 3.8 million tonnes of CO_2 were injected into the Krechba gas formation between August 2004 and June 2011, as part of the world's first demonstrative industrial-scale onshore CCS-project (Ma et al., 2022; Rinaldi et al., 2017). According to the interferometric synthetic-aperture radar (InSAR) measurements, about 5–10 mm of annual surface uplift was induced by the injection activity (Rinaldi and Rutqvist, 2013).

In general, the surface uplift is driven by the pore pressure increases in the injected formation, which can be estimated by a computational approach that couples the geomechanical response and formation characteristics with a numerical reservoir fluid flow model (Rinaldi et al., 2017; Rinaldi and Rutqvist, 2013; Rutqvist et al., 2010; Khan et al., 2018, 2020; Zheng et al., 2021; Siriwardane et al., 2016). Such studies require a rather complicated model setup with the heterogeneous properties of the target reservoirs, as well as the detailed production and injection data. Such analysis hinders quick decision-making processes due to its requirements of massive computational power and calculation time.

The Gaussian pressure transient (GPT) method (Weijermars, 2022a) is an analytical method to estimate the formation pore pressure distribution by production or injection from vertical or horizontal wells. If the analytical GPT-method is coupled with a geomechanical model describing the poroelastic response of the formation, the uplift and subsidence can be quantified analytically without suffering from the disadvantages of the more elaborate computational approaches. In addition, the method is grid-less and has a high resolution (See details in Appendix A and validation in Section 2.1). The GPT-method combined with the poroelastic response of the formation has not been performed before and its application to compute the geomechanical response during a CCS process is demonstrated in the present study for the first time.

In the present study, the newly proposed uplift analysis with the GPT-method is first validated by comparing the calculated results with the InSAR measurement of the Krechba gas field of In Salah. Next, the uplift was analyzed for two CCS-candidate fields in South Korea, i.e., the Pohang basin and the depleted Donghae gas reservoir. Combined with the geomechanical properties of the formation, we computed the pore pressure distribution as determined by the GPT-solution, interlinked with the estimation of the surface uplift and subsidence balance calculations.

2. Formation uplift determination with the GPT

In this study, the formation uplift during the CO_2-injection was analytically determined from the pore pressure change calculated by the GPT-method (Section 2.1). Then, the pore pressure change was combined with a geomechanical dilation model (Section 2.2). This approach, first presented in the present study, has not been tried before. Our proposed approach offers considerable advantages over existing modeling methods (See the review of prior art in Appendix A).

2.1. Gaussian pressure transient solution

The Gaussian Pressure Transient (GPT) method was recently derived by rigorously solving the pressure diffusion equation for 1D, 2D, and 3D cases (Weijermars, 2022a). The GPT-solution depicts the instantaneous reservoir pressure profile at any given time, as determined by the hydraulic diffusivity and the applied injection pressure as it interacts with the original reservoir pressure (See Appendix B for details).

Since the GPT-method only requires as inputs the well position, operating well bottomhole pressure (BHP), the hydraulic diffusivity values, and initial reservoir pressure. The time-dependent (transient) pore pressure changes can be determined by relatively simple analytical computations of the reservoir properties based on analytical expressions. The pressure transient can be spatially and temporarily evaluated throughout the reservoir space and is coupled with a poroelastic geomechanical response model. This approach allows for a rapid evaluation of the surface uplift for geological CO_2-storage candidate fields. In addition, only a limited number of essential input parameters are required and the analytical calculations are straightforward, making the GPT-method an effective tool for screening field injection candidates and making adjustment to the CCU injection design. The method is especially powerful when reservoir properties are only available as averages, without much detailed knowledge of the spatial variations in these data (e.g., during the early phase of geological CO_2-storage evaluation studies).

The GPT-solution was derived by solving the pressure diffusion equation and combining the pressure gradient solution with the Darcy flow equation (Weijermars, 2022a). A transient profile of the reservoir pressure can be computed for any time, t, and any arbitrary (x, y)-coordinate in a horizontal reservoir space, as fully determined by a series of GPT-solutions (Weijermars, 2022a). Next, a horizontal well with the lateral length of $2h_{len}$ is assumed to spatially solve the pressure gradients by the derivative of the GPT, assuming a homogeneous reservoir with infinite boundaries.

The pressure distribution, $P(x, y, t)$, everywhere in the reservoir at location (x,y) at any time, t, is given by (Weijermars, 2022a).

$$P(x,y,t) = P_0 + \sum_{k=1}^{n} \Delta P(x_k, y_k, t) \tag{1}$$

The change in the reservoir pressure, $\Delta P(x_k,y_k,t)$, in equation (1) can be summed for multiple, superposed pressure sources, and added to (in the case of injection) or subtracted from (in the case of extraction) the initial pressure, P_0, to calculate the resulting pressure distribution at any one time. Then, the differential value of the bottomhole pressure (BHP) and initial reservoir pressure (P_0) is multiplied by a properly scaled solution of the pressure transient probability function, $p(x, y, t)$ (Weijermars, 2022a):

$$\Delta P(x_k, y_k, t) = (\mathrm{BHP} - P_0) p(x, y, t) \tag{2}$$

The solution of the pressure transient probability function, $p(x, y, t)$, with the reservoir parameters incorporated via the hydraulic diffusivity, D, is presented in equation (3). It enables the representation of the pressure transient of formations with a uniform hydraulic diffusivity. The detailed derivation steps are presented in Weijermars (2022a).

$$p(x,y,t) = e^{-\left(\frac{x^2}{4Dt}\right)} \left[\frac{erf\left(\frac{y-h_{len}}{2\sqrt{Dt}}\right) - erf\left(\frac{y+h_{len}}{2\sqrt{Dt}}\right)}{2\, erf\left(\frac{h_{len}}{2\sqrt{Dt}}\right)} \right] \tag{3}$$

The hydraulic diffusivity, D, can be calculated from the principal reservoir parameters, such as permeability, k, porosity, Φ, fluid viscosity, μ, and total compressibility, c_t, and is determined by:

$$D = \frac{k}{\Phi \mu c_t} \tag{4}$$

Combining equations (1-3), we end up with equation (5), which quantifies the probabilistic pressure of the reservoir at any (x,y)-location at a given time, t. In addition, to carry out the pressure transient analysis of more complex cases containing multiple pressure sources, the unit

length term, x_{sp}, can be added to determine the spacing between each source.

$$P(x,y,t) = P_0 + (\mathrm{BHP} - P_0)\left[e^{-\left(\frac{x^2}{4Dt}\right)} + e^{-\left(\frac{(x-x_{sp})^2}{4Dt}\right)}\right]\left[\frac{erf\left(\frac{y-h_{len}}{2\sqrt{Dt}}\right) - erf\left(\frac{y+h_{len}}{2\sqrt{Dt}}\right)}{2\,erf\left(\frac{h_{len}}{2\sqrt{Dt}}\right)}\right] \quad (5)$$

2.2. Poroelastic response of the injected formation

According to Fjaer et al. (Fjær et al., 2008), the vertical displacement of a reservoir induced by the pore pressure change can be estimated with a few assumptions. First, Hooke's Law is introduced to correlate the elastic strain, ε, in three principal directions as a function of the principal stresses. Assuming linear poroelasticity of a homogeneous and isotropic reservoir, the relationship between changes in the effective principal in-situ stresses ($\Delta\sigma'_H$, $\Delta\sigma'_h$, and $\Delta\sigma'_v$), Young's modulus, E, Poisson's ratio, ν, and the principal strains can be expressed as equations (6-8).

$$E\varepsilon_H = \Delta\sigma'_H - \nu(\Delta\sigma'_h + \Delta\sigma'_v) \quad (6)$$

$$E\varepsilon_h = \Delta\sigma'_h - \nu(\Delta\sigma'_H + \Delta\sigma'_v) \quad (7)$$

$$E\varepsilon_v = \Delta\sigma'_v - \nu(\Delta\sigma'_H + \Delta\sigma'_h) \quad (8)$$

In most underground reservoir systems, the lateral width of the formation is far more elongated than its thickness. Thus, the horizontal strains are assumed to be zero. By combining the equations (6-8) accordingly, we get:

$$\Delta\sigma'_H = \Delta\sigma'_h = \frac{\nu}{1-\nu}\Delta\sigma'_v \quad (9)$$

Next, we regard the vertical strain, ε_v, to solely occur within the reservoir of thickness, h, and the vertical principal stress, σ'_v, acting on the formation top remains constant over time. Subsequently, pore pressure change, ΔP_f, of the reservoir only results in a vertical strain, ε_v. In addition, by multiplying the poroelastic coefficient term, a, to depict the mechanical transferability according to rock types, the relationship of equation (9) gives the amount of surface uplift Δh:

$$\Delta h = \frac{h}{E}\frac{(1+\nu)(1-2\nu)}{1-\nu}a\Delta P_f \quad (10)$$

2.3. Example

In this study, the pressure profile calculated using the GPT-solution method (Section 2.1) is combined with the formation dilation formula (Section 2.2) to analytically compute the pore pressure distribution during CO_2-injection along with the subsequent formation uplift and subsidence. When the formation is vertically dilated, both the overlying and underlying formations can be compacted. In addition, the upward deformation might be mitigated as it is transmitted to the surface. For simplicity and to adopt the worst-case scenario for design purposes, it was assumed that all the dilation of the formation will translate and result only in the upward deformation responsible for the surface uplift.

Fig. 1 shows the pore pressure profile and the subsequent uplift quantified after 1 month of CO_2-injection, for an artificial formation. The initial formation pressure, P_0, operating *BHP*, and the diffusivity coefficient, D, are assumed to be 10 MPa, 15 MPa, and 1 $m^2\ s^{-1}$ respectively. The h_{len} value was set as 0.0001 km for the vertical and 1.5 km for the horizontal well. The parameters were set to visualize the pressure and uplift profile of an example case describing the super critical phase CO_2 injection to a 1 km deep formation. It was shown that regardless of well types, a maximum uplift of 0.03 mm would occur after 1 month of CO_2-injection.

3. Validation (field case study): Krechba gas field

In this section, the uplift during the CO_2-injection in the Krechba gas field at In Salah (Algeria) was quantified using the GPT-method. At In

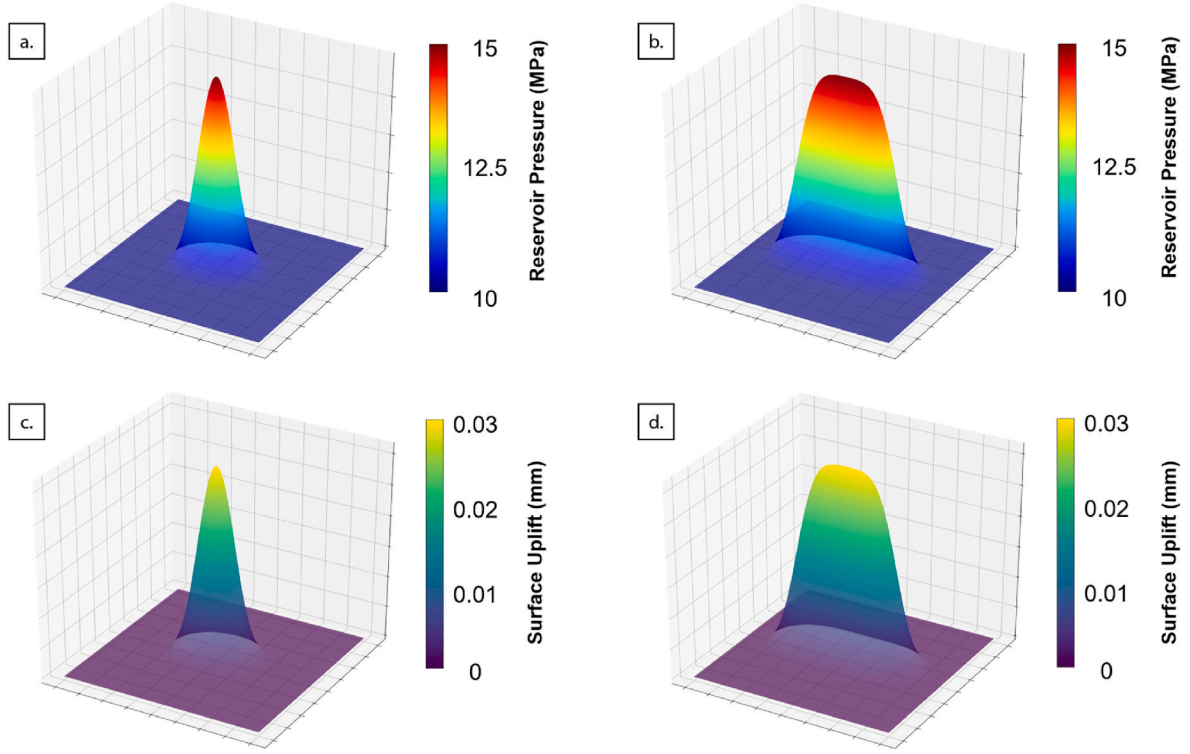

Fig. 1. (a, b) Pore pressure distribution and **(c, d)** the subsequent formation uplift during 1 month of CO_2-injection from vertical **(a, c)** and horizontal **(b, d)** wells.

Salah, between August 2004 and June 2011, about 0.5–1.0 million tonnes of CO_2 was annually injected through three 1.0–1.5 km long horizontal wells (Rinaldi et al., 2017; Rutqvist et al., 2010). Based on the InSAR satellite data, which is capable of measuring millimeter-scale surface deformation, it was found that 5–10 mm of annual uplift was detected during the first 3 years of the injection period (Rinaldi and Rutqvist, 2013).

The pore pressure distribution during the CO_2-injection in the Krechba gas field was determined by the GPT-solution method, equation **(5),** and the subsequent uplift was estimated by the dilation model, equation **(10)**. The results were compared with the InSAR data, to examine the validity of the GPT-analysis procedure. The input parameters of Table 1 were used in our model for the uplift analysis of the Krechba gas field.

Fig. 2a–c shows the surface uplift for a subsection of the In Salah field, as was monitored by the satellite-based InSAR data at one of the three horizontal wells of the Krechba gas field during the CO_2-injection period. The uplift was first sighted at the starred locations in Fig. 2a–c. The black lines in Fig. 2a–c indicate the KB-502 horizontal well that was used for injection in the actual project; it was also used in our models of Fig. 2d–f. After 11, 20, and 33 months of injection, the maximum uplift occurring at the location of the injection well was approximately 10, 15, and 14 mm, respectively (Table 2) (Rinaldi and Rutqvist, 2013). In addition, the uplifted area expanded and grew toward the northwestern area as the injection period was progressing.

The uplift calculated with the GPT-method are shown in Fig. 2d–f for comparison with the field data in Fig. 2a–c. Since it was assumed that the dilation calculated at the top of the underground formation is transmitted to the surface immediately, the maximum uplift of 14.22 mm is consistently predicted for all periods of injection, because it follows from the assumed pressure difference between the BHP and the initial reservoir pressure at the site of the well. However, as the injection proceeds, a larger region around the well will asymptotically attain the same maximum amount of uplift for that particular pressure (BHP).

The difference between the calculated and actual uplift is about 4.22 mm after 11 months of CO_2-injection. However, the difference diminishes for longer injection periods as the actual uplifts are increased to approximately 15 and 14 mm. The gap between the measured and the calculated data of the 11-month injection period implies that the dilation at the formation top at 1800 m depth was initially not transferred to the surface fully. After 20 months of injection, however, the surface uplift in the real field and as per our model differed only about 0.78 mm, which indicates that more formation dilation had been transferred to the surface. When the formation uplift was advanced after 33 months of injection, the difference between the GPT-calculation and the actual measurement reduced to 0.22 mm (Table 2).

The total area affected by the surface uplift due to the CO_2-injection in reality and as predicted by the GPT-method seems reasonably accurate for the 11 months of the injection period (Fig. 2). However, the uplifted surface area suggested by the GPT-analysis remains elliptical in shape, unlike the field example where innate heterogeneity of the formation affects the movement of the injection fluid, with a drift toward the northwest of the injection well. Such effects can in principle be accounted for by applying advanced GPT-methods, history-matching the surface uplift outline by using systematically changing anisotropic diffusivity parameters (Weijermars, 2022a), and examining the inclination of the formation, but such sensitivity studies were not further pursued here.

In conclusion, the GPT-model provides a very effective calculation of the actual surface uplift induced by the CO_2-injection. In terms of the maximum uplift, the prediction made by the GPT-model could accurately match the actual surface uplift observed at Krechba.

Table 1
Input parameters used for the analysis of the Krechba gas field (Rinaldi et al., 2017; Detournay and Cheng, 1993; Bjørnarå et al., 2018; Heidaryan et al., 2011).

Parameter	Value	Unit
Initial reservoir pressure	18.00	MPa
Injection well BHP	28.00	MPa
Reservoir thickness	20.00	m
Poisson's ratio	0.20	–
Young's modulus	10.00	GPa
Poroelastic coefficient	0.79	–
Permeability	8.00	md
Porosity	0.17	–
Bulk Modulus	7.94	MPa
Fluid viscosity	$3.40 \bullet 10^{-5}$	Pa•s
Rock compressibility	$1.26 \bullet 10^{-7}$	Pa^{-1}
Fluid compressibility	$6.90 \bullet 10^{-8}$	Pa^{-1}
Total compressibility	$1.16 \bullet 10^{-7}$	Pa^{-1}
Hydraulic Diffusivity	0.01	$m^2 \bullet s^{-1}$

4. Field applications: CCS-candidates in South Korea

In this section, the GPT-analysis was applied to predict the magnitude and visualize the spatial extent of the surface uplift for two CCS-candidate fields in South Korea, prior to the execution of the actual project. Both fields are anticipated to involve large injection volumes of CO_2-fluids. In addition, the subsidence of the surface is also taken into account by operating a relief well aimed at mitigating any excessive uplift. It is assumed in our assessment that the vertical deformation at the top of the formation is instantaneously transmitted to the surface without being dissipated in the overlying formation.

4.1. Pohang basin

The Pohang basin is the first pilot test site of CCS in South Korea (Fig. 3a and b), where a CO_2-injection well was drilled in 2017, and approximately 100 tonnes of CO_2 were injected into an aquifer (Kwon, 2018). Although no further injection plan has been established for the site, the basin still remains one of a few possible candidates for future CCS-projects in South Korea.

The anticipated surface uplift calculated with the GPT-method for the Pohang basin after 3, 6, and 12 months of CO_2-injection are depicted in Fig. 4a–c, respectively. Input parameters used for the calculation are described in Table 3. For the CCS-process in the Pohang basin, the optimal injection well location was established in a previous study by Song and Wang (2021).

In the GPT-model for the Pohang basin, the operating BHP of the injection well was assumed to be 14 MPa, which is the optimal injection pressure if the safe maximum storage capacity is targeted without reactivating the adjacent faults (Song and Wang, 2021). After 3 months of injection, the surface uplift (Fig. 4a) reaches the southeastern boundary of the formation. As the injection period is extended, the uplifted area widens. In addition, Fig. 4c shows that after a 1-year injection period, the entire aquifer is expected to be affected by upward deformation. A maximum uplift of 25.42 mm occurred at the location of the injection well for all periods of injection (For the reason explained in Section 3).

Next, it was assumed that a vertical relief well was operated with a lowered BHP of 5 MPa to mitigate the pore pressure increase due to the injection process. The optimal location of the relief well was determined according to a previous simulative study to achieve the maximum cumulative CO_2-injection volume without reactivating the closest fault around the injection well (Song and Wang, 2021). The study assured that the CO_2 breakthrough would not occur during a year of CO_2 injection. The optimized location of the relief well is separated horizontally by about 600 m from the injection well and occurs in the same formation as the injection well.

Fig. 4d–f shows that the uplift caused by the CO_2-injection can be mitigated by the extraction of formation fluid via the relief well. Moreover, with an operating relief well, the maximum uplift calculated

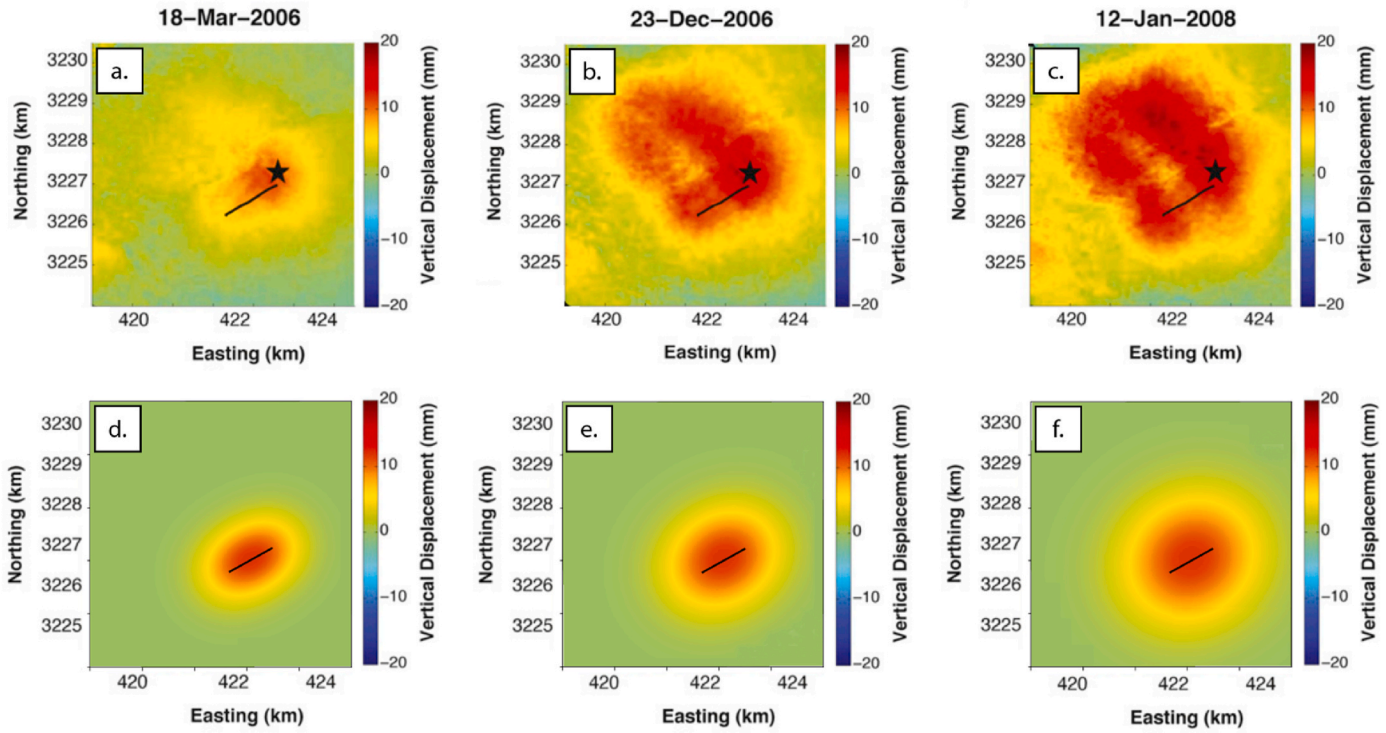

Fig. 2. (a–c) InSAR measurements of the Krechba gas field at 11, 20, and 33 months after the injection. Figures modified after Rinaldi, A. P. and Rutqvist, J. (Rinaldi and Rutqvist, 2013). (d–f) Surface uplift calculated with the GPT-method.

Table 2
Maximum uplifts in the Krechba gas field measured by InSAR (Rinaldi and Rutqvist, 2013) and calculated with the GPT-method.

Time after injection (months)	Uplift by InSAR (mm)	Uplift by GPT (mm)	Difference between InSAR and GPT (mm)
11	10.00	14.22	4.22
20	15.00	14.22	0.78
33	14.00	14.22	0.22

at the location of the injection well is 22.34, 20.24, and 18.51 mm after 3, 6, and 12 months of the operation, respectively. In addition, the maximum subsidence calculated at the location of the relief well is also mitigated and is −5.05, −2.62, and −0.90 mm after 3, 6, and 12 months of operation, respectively (Table 4). Consequently, operating a relief well is a very effective method for mitigating the uplift caused by the CO_2-injection. Operating a relief well causes formation subsidence and the magnitude decreases as the operating period is extended.

4.2. *Donghae gas reservoir*

The depleted Donghae gas reservoir is located in the East Sea, 58 km from the city of Ulsan, Korea (Fig. 5a and b). The reservoir was produced from January 2005 to February 2022 and is projected to be repurposed for CCS. The input parameters of Table 5 were used for the uplift analysis of the Donghae gas reservoir.

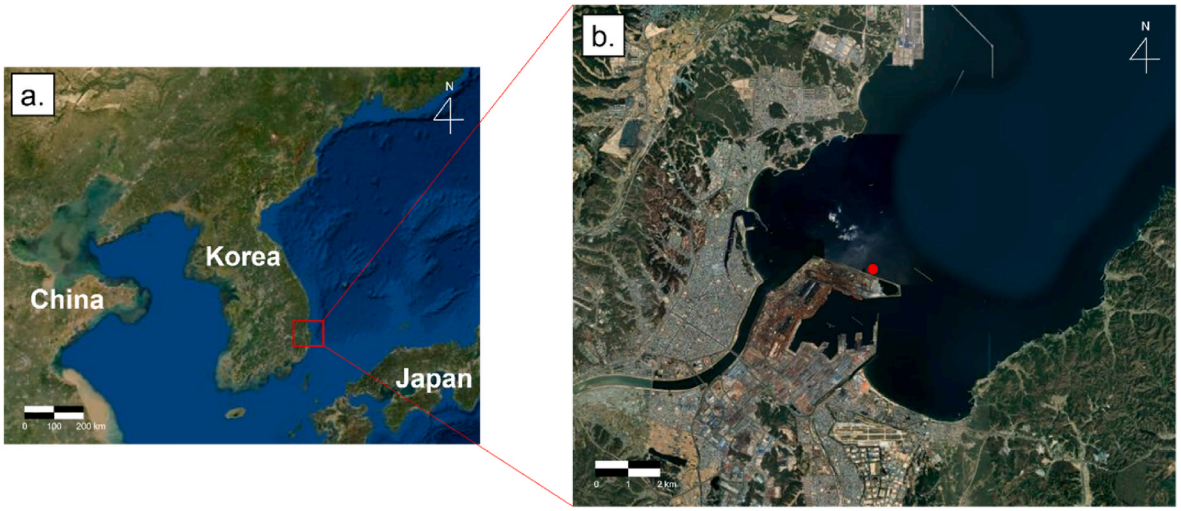

Fig. 3. (a) Location of the Pohang basin in the South Korean peninsula (b) Enlarged map of the Pohang basin area. Red dot indicates the currently drilled injection well. (For interpretation of the references to colour in this figure legend, the reader is referred to the Web version of this article.)

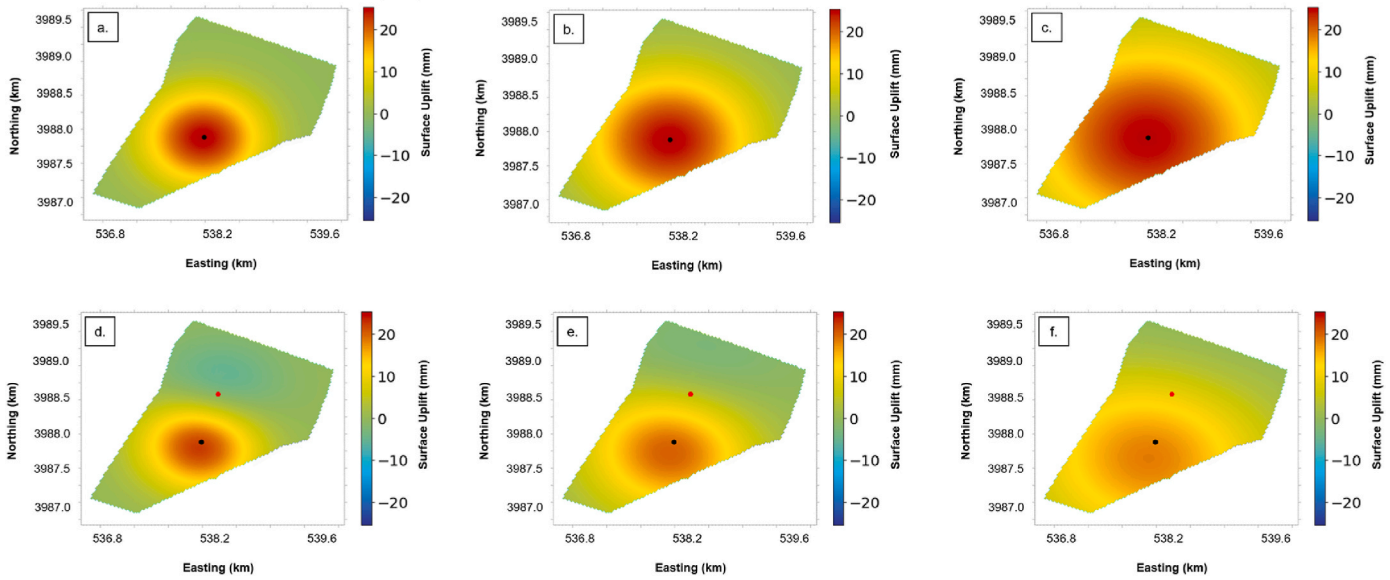

Fig. 4. Uplift calculated by the GPT-method in the Pohang basin: (a–c) 3, 6, and 12 months after injection without a relief well; (d–f) injection with a relief well, after 3, 6, and 12 months. Black and red dots represent the locations of the injection well and the relief well, respectively. (For interpretation of the references to colour in this figure legend, the reader is referred to the Web version of this article.)

Table 3
Input parameters used for the analysis of Pohang basin (Rinaldi et al., 2017; Detournay and Cheng, 1993; Bjørnarå et al., 2018; Heidaryan et al., 2011; Song and Wang, 2021; Kim et al., 2013; Kim et al., 2018).

Parameter	Value	Unit
Initial reservoir pressure	7.50	MPa
Injection well BHP	14.00	MPa
Relief well BHP	5.00	MPa
Reservoir thickness	11.00	m
Poisson's ratio	0.20	–
Young's modulus	2.00	GPa
Poroelastic coefficient	0.79	–
Permeability	30.00	md
Porosity	0.20	–
Bulk Modulus	7.94	MPa
Fluid viscosity	$3.40 \bullet 10^{-5}$	Pa•
Rock compressibility	$1.26 \bullet 10^{-7}$	Pa^{-1}
Fluid compressibility	$6.90 \bullet 10^{-8}$	Pa^{-1}
Total compressibility	$1.15 \bullet 10^{-7}$	Pa^{-1}
Hydraulic Diffusivity	0.04	$m^2 \bullet s^{-1}$

Table 4
Maximum uplift and subsidence in Pohang basin calculated by the GPT-method.

Time after operation (months)	Without relief well	With relief well	
	Uplift (mm)	Uplift (mm)	Subsidence (mm)
3	25.42	22.34	−5.05
6	25.42	20.24	−2.62
12	25.42	18.51	−0.90

Assuming an injection well located at the center of the reservoir, the uplifts induced by the CO_2-injection were calculated and are shown in Fig. 6a–c. The operating BHP of 35.02 MPa was determined by Sung et al. (2011), who suggested an optimal design scheme to effectively inject CO_2 into the reservoir.

The predicted maximum uplift at the well site, due to the BHP, is 25.42 mm for all 3, 6, and 12 months of injection (Table 6). In addition, the uplifted area will expand as the injection period lengthens (Fig. 6a–c).

In order to investigate the effect of operating a relief well, it was assumed that a well is located about 700 m southeast of the injection well and is producing the formation fluid for the same formation as the injection target with the BHP of 15 MPa. Fig. 6d–f, show that the uplift induced by the CO_2-injection is mitigated by the operation of the relief well. In addition, the calculated values (Table 6) show that the production of formation fluid by the relief well induces localized subsidence in the formation. The uplift and subsidence after 3 months of operation are 25.48 and −23.93 mm, respectively, which are reduced to 15.08 and −13.49 mm after 12 months of operation. The magnitudes of both uplift and subsidence decrease as the operating period is extended. It is suggested that a long-term stabilization and control of the surface uplift and subsidence for the Donghae gas reservoir is possible.

The uplift analysis with the GPT-model for both the Pohang basin and Donghae gas reservoir has demonstrated the applicability of the proposed method for predicting the uplift and subsidence of the CCS-target formations. By quantifying the impact of operating a relief well, it appeared that operating such relief well provides a very effective method to mitigate the formation uplift, while local subsidence remains limited. Consequently, the uplift and subsidence analysis with the GPT-method as first applied in the present study, based on earlier derivations of the pressure transient (See Appendix B), can be effectively adopted for computing both the formation uplift and subsidence. Our results suggest that long-term reservoir stabilization designs can rapidly be evaluated to avoid the occurrence of unwarranted geomechanical effects and hazards.

5. Discussion

In this study, the GPT-method (Weijermars, 2022a) was coupled with a geomechanical model and applied to determine the pore pressure changes during CO_2-injection and to evaluate the subsequent formation uplift and subsidence. According to the In Salah field observations, the measured surface uplifts indicated a non-uniform uplift distribution. We attribute the observed asymmetry to reservoir heterogeneity, which creates spatial variance of the pore pressure buildup. Although the proposed GPT-method as applied in this study did not take into account the reservoir heterogeneity, its applicability for the preliminary analysis in the early stages of the field exploitation is evident from the close convergence of the model outcomes and the actual field data. The

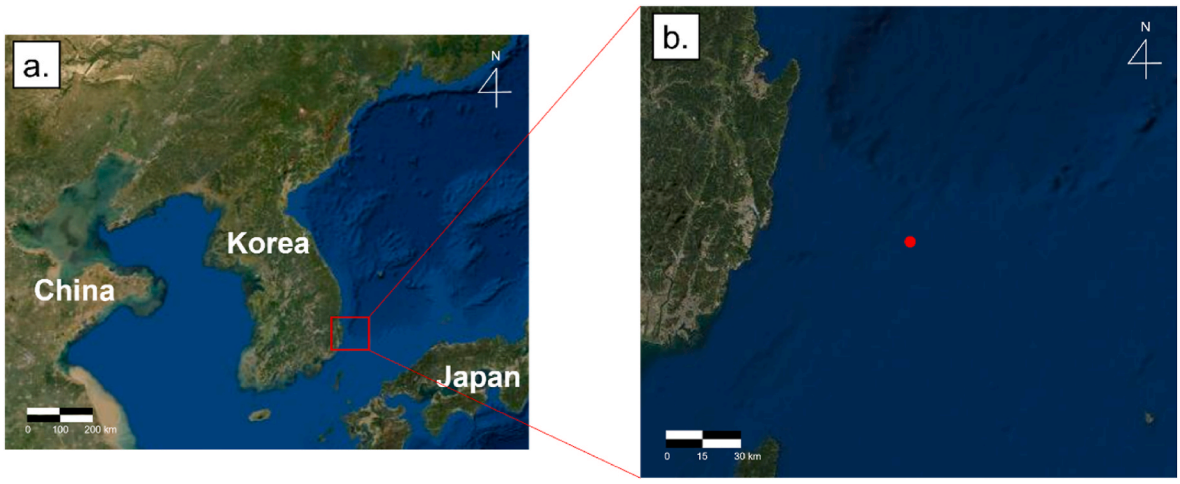

Fig. 5. (a) Location of the Donghae gas reservoir in the South Korean peninsula. **(b)** Enlarged map of the Donghae gas reservoir area. Red dot indicates the offshore location of the gas reservoir. (For interpretation of the references to colour in this figure legend, the reader is referred to the Web version of this article.)

Table 5
Input parameters used for the analysis of the Donghae gas reservoir (Rinaldi et al., 2017; Detournay and Cheng, 1993; Bjørnarå et al., 2018; Sung et al., 2011).

Parameter	Value	Unit
Initial reservoir pressure	24.80	MPa
Injection well BHP	35.02	MPa
Relief well BHP	15	MPa
Reservoir thickness	56.00	m
Poisson's ratio	0.20	–
Young's modulus	12.50	GPa
Poroelastic coefficient	0.79	–
Permeability	50.00	md
Porosity	0.16	–
Bulk Modulus	7.94	MPa
Fluid viscosity	$3.40 \bullet 10^{-5}$	Pa•s
Rock compressibility	$1.26 \bullet 10^{-7}$	Pa^{-1}
Fluid compressibility	$6.90 \bullet 10^{-8}$	Pa^{-1}
Total compressibility	$1.15 \bullet 10^{-7}$	Pa^{-1}
Hydraulic Diffusivity	0.08	$m^2 \bullet s^{-1}$

maximum uplift values at the location of the injection well appeared to give satisfactory close matches (Table 2).

5.1. Model strengths and limitations

When a formation is vertically inflated by its poroelastic response to pore-pressure buildup, it might dilate both upwards, downwards, and

Table 6
Maximum uplift and subsidence in the Donghae gas reservoir calculated by the GPT-method.

Time after operation (months)	Without relief well	With relief well	
	Uplift (mm)	Uplift (mm)	Subsidence (mm)
3	32.55	25.48	−23.93
6	32.55	20.01	−18.43
12	32.55	15.08	−13.49

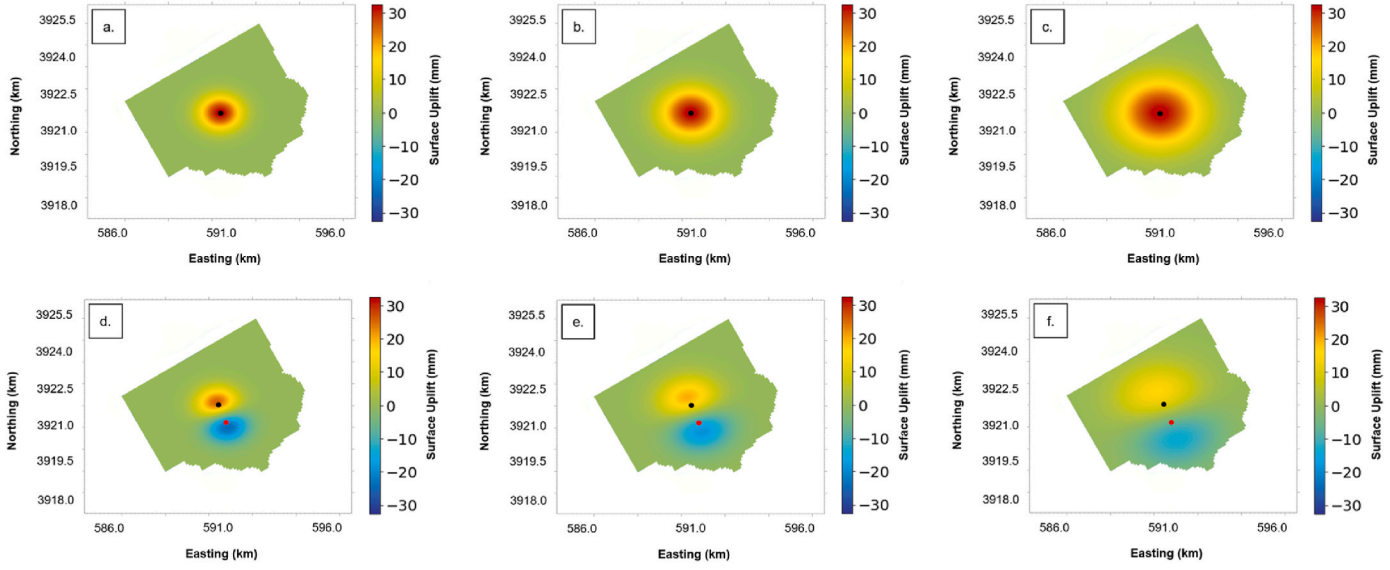

Fig. 6. Uplift calculated by the GPT-method in the Donghae gas reservoir: **(a–c)** 3, 6, and 12 months after injection without a relief well; **(d–f)** injection with a relief well, after 3, 6, and 12 months. Black and red dots represent the locations of the injection well and the relief well, respectively. (For interpretation of the references to colour in this figure legend, the reader is referred to the Web version of this article.)

sideways. In this study, it was assumed that all deformation would occur to the upward direction of the target formation only to calculate the maximum uplift expected due to CO_2 injection (limiting the lateral strain of the near wellbore region).

In this study, it was further assumed that the uplift and subsidence at the top of the injected formation are transmitted to the surface, instantaneously, without any time lag and attenuation. For the design purposes, the assumption seems quite reasonable for estimating the worst-case scenario uplift due to an elastic response; in fact, an instantaneous elastic response model seems adequate, so no compelling reasons exist to include adjustments for the anelastic response, in spite of some indication that a time lag would occur in the early months of injection (See section 3) before the full elastic response transmits to the surface.

The strength of the GPT-method presented in the study is that it necessitates only a few properties such as the BHP, Young's modulus, porosity, and permeability. The straightforwardness of the method enables quick analytical predictions of the expected surface uplift at the early stages of the CO_2 injection, but it also neglects the uncertainty within the properties as they are assumed as constants. For example, when injecting CO_2 into the reservoir, the BHP would fluctuate due to injection scheme changes and facility limitations. In addition, Young's modulus, Poisson's ratio, and permeability are also dynamic properties with uncertainties (Bao and Burghardt, 2022). For the case of a preliminary analysis predicting the worst-case scenario of surface uplift, the GPT-method presented is plausible, however for more sophisticated research, the uncertainties of the mentioned properties should be taken into consideration.

However, if the uplift analysis with the GPT-method is to be adopted to fields containing discontinuities, the potential reactivation of existing faults needs to be investigated, which can be induced by the pore pressure buildup during the CCS process. If the reservoir pore pressure exceeds the maximum allowable pressure determined by the properties of the faults and the in-situ stress conditions, the fault reactivation can occur. Therefore, the maximum allowable pressure and operating BHP should be determined for the safe and stable CCS process.

Our analysis showed that the upward deformation may be mitigated by drilling a pressure-relief well. To quantitatively estimate the attenuation ratio of the uplift, the deformation and the poroelastic response of the overlying formation during the CCS-period need to be reliably measured. However, if there is no pressure communication between overlying formations, changes in pore pressure cannot be transmitted vertically. A case study of fracture hits during hydraulic fracturing of the Eagle Ford formation into the overlying Austin Chalk has shown, that after the completion of the hydraulic fracturing, the original formation pressure in the Eagle Ford was maintained, while the Austin Chalk was already pressure depleted (Sukumar et al., 2019). In other words, pressure communication across formation boundaries with all their clay intercalations sealing off individual target zones is very unlikely to occur. In addition, the deformation assumed by the GPT-method is elastic regardless of time. However, for the geomechanical risk analysis of CO_2 injection, the viscoelastic time dependent deformation should also be considered not to underestimate the risks (Bao et al., 2021).

5.2. Future work

Several directions for future extension of the approach advocated in this study are possible. For example, the impact of uncertainty in input parameters can be readily accounted for by transforming the model from a deterministic one into a probabilistic one. Such a model transformation is straightforward, because the set of algorithms uses only analytical equations, which allow for input of probabilistic distribution functions (for certain key input parameters with high uncertainty) and then produce probabilistic outputs. Separately, a viscoelastic and time-dependent deformation model can be coupled with the GPT analysis, which will be subject of a future study.

6. Conclusion

In this study, possible uplift rates of anticipated CCS-projects were quantified and visualized by the GPT-method. The primary conclusions from this study are as follows.

1. During CCS by CO_2-injection, pressure increase in the formation is unavoidable, and surface uplift will occur due to the pore pressure buildup in the porous target reservoirs. The GPT-method was applied to calculate the pore pressure distribution and the subsequent formation uplifts that would occur during CCS-projects, assuming homogenous reservoir properties and a constant BHP for the injection well(s).
2. The observed surface uplift during CO_2-injection in the Krechba gas field at In Salah, Algeria, was correctly predicted by the proposed method. The results show that the maximum uplift in the model and observed rate at the location of the injection well only differed by 0.22 mm after 33 months of injection. In addition, the uplifted area expanded as the injection period continued, for both measured and calculated results.
3. Applying the GPT method to the CCS-candidate sites of South Korea, the surface uplift in the Pohang basin and the Donghae gas reservoir was quantified in a preliminary assessment of the possible effects due to the injection process. Additionally, the impact was assessed by operating relief wells that would mitigate the formation uplift, which eased the increment of the pore pressure in the formation. Although some subsidence was observed at the locations of the relief wells, the magnitude of both the uplift and subsidence decreased as the operation period is extended.
4. It was concluded that the GPT-method can be reliably used to compute the formation pore pressure distribution and the subsequent formation uplift and subsidence. Due to its straightforwardness, its applicability is extremely useful in the CCS-development design phase, including the evaluation of the most effective well types, well locations, and well operating conditions.

Credit author statement

Sungjun Jun: Methodology, Software, Investigation, Data Curation, Writing - Original Draft; **Youngsoo Song**: Validation, Resources, Formal analysis; **Jihoon Wang**: Conceptualization, Writing - Review & Editing, Supervision, Project administration, Funding acquisition; **Ruud Weijermars**: Writing - Review & Editing.

Declaration of competing interest

The authors declare that they have no known competing financial interests or personal relationships that could have appeared to influence the work reported in this paper.

Data availability

The data that has been used is confidential.

Acknowledgments

This work was supported by the research fund of Hanyang University (HY-2020) and was supported by the Korea Institute of Energy Technology Evaluation and Planning(KETEP) and the Ministry of Trade, Industry & Energy (MOTIE) of the Republic of Korea (No. 20214710100060).

Appendix A. Prior Art for Modeling Surface Uplift and Subsidence

Fluid injection into the underground formations has been executed worldwide in the recent centuries for multiple purposes, e.g., enhanced oil recovery (EOR), aquifer storage and recharge (ASR), carbon gas storage, surface subsidence mitigation, geomechanical characterization, etc. (Teatini et al., 2011). Thus, the accuracy of the computational model is very crucial to reliably design the injection process.

Numerical Models

The formation deformation in response to the pore pressure changes are normally analyzed and predicted by combining a numerical multiphase flow simulator and a geomechanical simulator. The pair of TOUGH2-FLAC3D has been widely adopted for the delineation of ground surface deformation at the In Salah CCS-field site due to the CO_2-injection at the Krechba gas field, Algeria. The studies (Rinaldi and Rutqvist, 2013; Rutqvist et al., 2010) could successfully history-match the uplift due to the CO_2-injection with the coupled model, by setting the satellite-measured InSAR data as the standard. Studies of the same objective have also been inversely carried out with the parameter estimation model of iTOUGH2 to optimize the results (Rinaldi et al., 2017).

The reservoir simulator of Computer Modeling Group (CMG) provides another option to couple the fluid flow simulator, GEM, with a geomechanical model using a gridded numerical solution scheme. Various studies (Khan et al., 2018, 2020; Zheng et al., 2021; Siriwardane et al., 2016) used the CMG-model to generate and predict the relationship between the formation characteristics with the vertical ground displacement.

As aforementioned, numerical simulators are capable of constructing and modeling the target formations while accounting for incorporated heterogeneities of the thermal, hydraulic, and mechanical behaviors. In addition, when coupled with adequate geomechanical simulators, in-depth geomechanical analysis of the fields is possible. However, to fully benefit from the capacity of such advanced modeling approaches, a large number of input parameters and their spatial variation are required. The availability of such detailed subsurface data is often lacking, especially in the early stages of CCS-project evaluation studies. In addition, massive computing time and high-performance computing capabilities (Rutqvist, 2011) make such projects costly and time-consuming, while precluding rapid iterations for optimization of field development solutions. This explains the primary motivation for us to propose, develop and demonstrate the practicality of applying the GPT-solutions in CCS-project assessment studies.

Analytical Models

An analytical model for subsidence estimations in a certain production horizon with a cylindrical boundary proposed by Geertsma, 1973a, 1973b was based on Bessel function integrals and uniform pressure draw-down in a bounded reservoir space. The model uses a strain-nucleus concept and compatibility equations to solve for the subsidence due to an assumed uniform pressure drop in a producing formation. The Geertsma-model has been widely applied in subsidence studies as a pore compaction process (Van Thienen-Visser and Fokker, 2017; Zoback, 2007), and could equally be applied in uplift studies (But no such direct applications are known to the authors). However, the Geertsma-model is not accounting for the physics of pressure migration from the origin of the engineering intervention; it assumes a uniform pressure drop has occurred throughout the cylindrical reservoir space, which is then used in the nucleus-of-strain solution method to compute the profile of the subsidence. There is no time-dependency in the equations, and the uniform pressure drop is an input that would need justification from a reservoir pressure-depletion model. In addition to those constraints, the Geertsma-model is deemed rather complex but can be simplified (Zoback, 2007). The GPT-method proposed in the present study follows an entirely different analytical solution path, and therefore cannot be compared directly with solutions based on the Geertsma-model.

Appendix B. Development of the GPT-method and technical details

Analysis of the formation deformation by the pore pressure change with the GPT-method presented in this study contains a strength in its straightforwardness. Since it assumes homogeneous formation characteristics and requires only a few essential input parameters (The well position, the operating BHP, and the hydraulic diffusivity), the method is capable of analytically solving the pressure diffusion equation of any injection or production scheme at any given time.

The pressure diffusion equation was solved analytically as a function of the imposed bottomhole pressure only, without reference to the well rate, for the first time by Weijermars (2022a), using a Gaussian pressure transient (GPT). Previously, the only available solution for the pressure transient, used in well-testing studies, was based on Thiem (1887), and it required both the bottomhole pressure and the well rate as inputs. The new GPT-solution accurately predicts the advance of the pressure-depletion zone in space and time, based on the pressure transient equation (Fjær et al., 2008). The transient representing the time-dependent pore pressure change can be rapidly determined with the GPT-equations (Weijermars, 2022a; Fjær et al., 2008).

The probabilistic pressure of the reservoir at any *(x,y)* location at any given time, *t*, given by the GPT (Weijermars, 2022a) is:

$$P(x,y,t) = P_0 + (\mathrm{BHP} - P_0)\, e^{-\left(\frac{r^2}{4Dt}\right)} \left[\frac{erf\left(\frac{y-h_{len}}{2\sqrt{Dt}}\right) - erf\left(\frac{y+h_{len}}{2\sqrt{Dt}}\right)}{2\, erf\left(\frac{h_{len}}{2\sqrt{Dt}}\right)} \right] \tag{B.1}$$

The transient pore pressure change, Δp_f, of the formation is then equated with the difference between $P(x,y,t)$ and P_0 (Weijermars, 2022a; Fjær et al., 2008):

$$\Delta P_f = P(x,y,t) - P_0 \tag{B.2}$$

The vertical displacement equation derived by Fjaer et al. (Fjær et al., 2008) is used to quantify the surface uplift analytically:

$$\Delta h = \frac{h}{E} \frac{(1+v)(1-2v)}{1-v} a \Delta P_f \tag{B.3}$$

Equations B.2 and B.3 are combined to get the final analytical equation used hereinbefore to quantify the uplift by the GPT-method (Equation B.5).

$$\Delta h = \frac{h}{E}\frac{(1+v)(1-2v)}{1-v}a[P(x,y,t)-P_0] \tag{B.4}$$

$$\Delta h = \frac{h}{E}\frac{(1+v)(1-2v)}{1-v}a\left\{\left\{P_0+(\mathrm{BHP}-P_0)\,e^{-\left(\frac{x^2}{4Dt}\right)}\left[\frac{erf\left(\frac{y-h_{len}}{2\sqrt{Dt}}\right)-erf\left(\frac{y+h_{len}}{2\sqrt{Dt}}\right)}{2\,erf\left(\frac{h_{len}}{2\sqrt{Dt}}\right)}\right]\right\}-P_0\right\} \tag{B.5}$$

While the present paper focuses on the application of the GPT-method (Weijermars, 2022a; Fjær et al., 2008) to quantify the surface uplift and subsidence caused by engineered pore pressure changes, other applications include the prediction of principal stress changes near hydraulic fractures due to production-induced pressure depletion (Wang and Weijermars, 2022; Weijermars and Wang, 2021), and field-based estimations of the hydraulic diffusivity of shale formations using a Gaussian decline curve analysis (DCA) method (Weijermars, 2022b; Weijermars and Afagwu, 2022), which is faster and more accurate than Arps-based history matches of the well rate. In addition, the GPT-method can be used as a reservoir simulator for fluid migration near hydraulically fractured well systems (Afagwu and Weijermars, 2022).

7. References

Afagwu, C., Weijermars, R., 2022. Gaussian simulator of multi-fractured well production performance. Frontiers submitted for publication).

Appriou, D., 2019. Assessment of the Geomechanical Risks Associated with CO2 Injection at the FutureGen 2.0 Site. US Department of Energy. https://doi.org/10.2172/1594048.

Bao, T., Burghardt, J., 2022. A bayesian approach for in-situ stress prediction and uncertainty quantification for subsurface engineering. Rock Mech. Rock Eng. 1–18. https://doi.org/10.1007/s00603-022-02857-0.

Bao, T., Burghardt, J., Gupta, V., White, M., 2021. Impact of time-dependent deformation on geomechanical risk for geologic carbon storage. Int. J. Rock Mech. Min. Sci. 148, 104940 https://doi.org/10.1016/j.ijrmms.2021.104940.

Bjørnarå, T.I., Bohloli, B., Park, J., 2018. Field-data analysis and hydromechanical modeling of CO2 storage at in Salah, Algeria. Int. J. Greenh. Gas Control 79, 61–72. https://doi.org/10.1016/j.ijggc.2018.10.001.

Cao, M., Sharma, M.M., 2022a. Factors controlling the flow and connectivity in fracture networks in naturally fractured geothermal Formations. SPE Drill. Complet. 1–15. https://doi.org/10.2118/212292-PA.

Cao, M., Sharma, M.M., 2022b. The impact of changes in natural fracture fluid pressure on the creation of fracture networks. J. Petrol. Sci. Eng. 216, 110783 https://doi.org/10.1016/j.petrol.2022.110783.

Cappa, F., Rutqvist, J., 2011. Modeling of coupled deformation and permeability evolution during fault reactivation induced by deep underground injection of CO2. Int. J. Greenh. Gas Control 5, 336–346. https://doi.org/10.1016/j.ijggc.2010.08.005.

Detournay, E., Cheng, A.H.-D., 1993. Fundamentals of poroelasticity. Chapter 5 in comprehensive rock engineering: principles. Practice and Projects 2, 113–171.

Donovan, D.J., Katzer, T., Brothers, K., Cole, E., Johnson, M., 2002. Cost-benefit analysis of artificial recharge in las vegas valley, Nevada. J. Water Resour. Plann. Manag. 128 https://doi.org/10.1061/(ASCE)0733-9496(2002)128:5(356).

Ferronato, M., Gambolati, G., Janna, C., Teatini, P., 2010. Geomechanical issues of anthropogenic CO2 sequestration in exploited gas fields. Energy Convers. Manag. 51, 1918–1928. https://doi.org/10.1016/j.enconman.2010.02.024.

Fjær, E., Holt, R., Horsrud, P., Raaen, A., 2008. Petroleum Related Rock Mechanics, second ed. Elsevier.

Geertsma, J.A., 1973a. Basic theory of subsidence due to reservoir compaction: the homogeneous case. Verhandelingen Koninklijk Nederlandsch Geologisch Mijnbowkundig Genootschap 23, 43–61.

Geertsma, J.A., 1973b. Land subsidence above compacting oil and gas reservoirs. J. Petrol. Technol. 734–744. https://doi.org/10.2118/3730-PA.

Heidaryan, E., Hatami, T., Rahimi, M., Moghadasi, J., 2011. Viscosity of pure carbon dioxide at supercritical region: measurement and correlation approach. J. Supercrit. Fluids 56, 144–151. https://doi.org/10.1016/j.supflu.2010.12.006.

Hoffmann, J., Zebker, H.A., Galloway, D.L., Amelung, F., 2001. Seasonal subsidence and rebound in las vegas valley, Nevada, observed by synthetic aperture radar interferometry. Water Resour. Res. 37, 1551–1566. https://doi.org/10.1029/2000WR900404.

Khan, S., Khulief, Y.A., Al-Shuhail, A., 2018. Mitigating climate change via CO2 sequestration into Biyadh reservoir: geomechanical modeling and caprock integrity. Mitig. Adapt. Strategies Glob. Change 24, 23–52. https://doi.org/10.1007/s11027-018-9792-1.

Khan, S., Khulief, Y., Al-Shuhail, A., Bashmal, S., Iqbal, N., 2020. The geomechanical and fault activation modeling during CO2 injection into deep minjur reservoir, eastern Saudi arabia. Sustainability 12. https://doi.org/10.3390/su12239800.

Kim, H., Song, I., Chang, C., Lee, H., Kim, T., 2013. Relations between physical and mechanical properties of core samples from the bukpyeong and Pohang basins. J. Eng. Geol. 23, 329–340. https://doi.org/10.9720/kseg.2013.4.329.

Kim, S.K., Chang, C., Shinn, Y., Kwon, Y., 2018. Characteristics of Pohang CO2 geological sequestration test site. J. Eng. Geol. 28 https://doi.org/10.9720/kseg.2018.2.175.

Kim, H., McJeon, H., Jung, D., Lee, H., Bergero, C., Eom, J., 2022. Integrated assessment modeling of korea's 2050 carbon neutrality technology pathways. Energy and Climate Change 3. https://doi.org/10.1016/j.egycc.2022.100075.

Kresse, O., Weng, X., 2018. Numerical modeling of 3D hydraulic fractures interaction in complex naturally fractured formations. Rock Mech. Rock Eng. 51, 3863–3881. https://doi.org/10.1007/s00603-018-1539-5.

Kwon, Y.K., 2018. Demonstration-scale offshore CO2 storage project in the Pohang basin, Korea. J. Eng. Geol. 28 https://doi.org/10.9720/kseg.2018.2.133.

Li, C., Barès, P., Laloui, L., 2015. A hydromechanical approach to assess CO2 injection-induced surface uplift and caprock deflection. Geomechanics for Energy and the Environment 4, 51–60. https://doi.org/10.1016/j.gete.2015.06.002.

Ma, J., Li, L., Wang, H., Du, Y., Ma, J., Zhang, X., et al., 2022. Carbon capture and storage: history and the road ahead. Engineering. https://doi.org/10.1016/j.eng.2021.11.024.

Nicol, A., Carne, R., Gerstenberger, M., Christophersen, A., 2011. Induced seismicity and its implications for CO2 storage risk. Energy Proc. 4, 3699–3706. https://doi.org/10.1016/j.egypro.2011.02.302.

Rinaldi, A.P., Rutqvist, J., 2013. Modeling of deep fracture zone opening and transient ground surface uplift at KB-502 CO2 injection well, in Salah, Algeria. Int. J. Greenh. Gas Control 12, 155–167. https://doi.org/10.1016/j.ijggc.2012.10.017.

Rinaldi, A.P., Rutqvist, J., Finsterle, S., Liu, H.-H., 2017. Inverse modeling of ground surface uplift and pressure with iTOUGH-PEST and TOUGH-FLAC: the case of CO2 injection at in Salah, Algeria. Comput. Geosci. 108, 98–109. https://doi.org/10.1016/j.cageo.2016.10.009.

Roberts, J.J., Stalker, L., Shipton, Z.K., Burnside, N.M., 2018. What have we learnt about CO2 leakage in the context of commercial-scale CCS?. In: 14th International Conference on Greenhouse Gas Control Technologies, GHGT-14 https://doi.org/10.2139/ssrn.3366113.

Rutqvist, J., 2011. Status of the TOUGH-FLAC simulator and recent applications related to coupled fluid flow and crustal deformations. Comput. Geosci. 37, 739–750. https://doi.org/10.1016/j.cageo.2010.08.006.

Rutqvist, J., Vasco, D.W., Myer, L., 2010. Coupled reservoir-geomechanical analysis of CO2 injection and ground deformations at in Salah, Algeria. Int. J. Greenh. Gas Control 4, 225–230. https://doi.org/10.1016/j.ijggc.2009.10.017.

Siriwardane, H.J., Gondle, R.K., Varre, S.B., Bromhal, G.S., Wilson, T.H., 2016. Geomechanical response of overburden caused by CO 2 injection into a depleted oil reservoir. J. Rock Mech. Geotech. Eng. 8, 860–872. https://doi.org/10.1016/j.jrmge.2016.06.009.

Song, Y., Wang, J., 2021. Optimization of relief well design using artificial neural network during geological CO2 storage in Pohang basin, South Korea. Appl. Sci. 11 https://doi.org/10.3390/app11156996.

Sukumar, S., Weijermars, R., Alves, I., Noynaert, S., 2019. Analysis of pressure communication between the Austin Chalk and Eagle Ford reservoirs during a zipper fracturing operation. Energies 12. https://doi.org/10.3390/en12081469.

Sun, R.J., 1969. Theoretical size of hydraulically induced horizontal fractures and corresponding surface uplift in an idealized medium. J. Geophys. Res. 74, 5995–6011. https://doi.org/10.1029/JB074i025p05995.

Sung, W.M., Lee, Y.S., Kim, K.H., Jang, Y.H., Lee, J.H., Yoo, I.H., 2011. Investigation of CO2 behavior and study on design of optimal injection into Gorae-V aquifer. Environ. Earth Sci. 64, 1815–1821. https://doi.org/10.1007/s12665-011-1001-4.

Teatini, P., Gambolati, G., Ferronato, M., Settari, A., Walters, D., 2011. Land uplift due to subsurface fluid injection. J. Geodyn. 51, 1–16. https://doi.org/10.1016/j.jog.2010.06.001.

Thiem, A., 1887. Verfahress für Natürlicher Grundwassergeschwindegkiten (Movement of natural groundwater flow). Polytechnisches Notizblatt 42, 229.

Van Thienen-Visser, K., Fokker, P.A., 2017. The future of subsidence modelling: compaction and subsidence due to gas depletion of the Groningen gas field in The Netherlands. Neth. J. Geosci. 96, s105–s116.

Wang, J., Weijermars, R., 2022. Production-induced pressure-depletion and stress anisotropy changes near hydraulically fractured wells: implications for intra-well fracture interference and fracture treatment efficacy. J. Petrol. Sci. Eng. submitted for publication).

Wei, Y., Maroto-Valer, M., Steven, M.D., 2011. Environmental consequences of potential leaks of CO2 in soil. Energy Proc. 4, 3224–3230. https://doi.org/10.1016/j.egypro.2011.02.239.

Weijermars, R., 2022a. Production rate of multi-fractured wells modeled with Gaussian pressure transients. J. Petrol. Sci. Eng. 210 https://doi.org/10.1016/j.petrol.2021.110027.

Weijermars, R., 2022b. Gaussian Decline Curve Analysis Method: A Fast Tool for Analyzing Hydraulically Fractured Wells in Shale Plays Demonstrated with Examples from HFTS-1 (Hydraulic Fracture Test Site-1, Midland Basin, West Texas). MDPI Energies, 2022, in review.
Weijermars, R., Afagwu, C., 2022. Hydraulic diffusivity estimations for US shale gas reservoirs with Gaussian method: implications for pore-scale diffusion processes in underground repositories. J. Nat. Gas Sci. Eng. (in press).
Weijermars, R., Wang, J., 2021. Stress reversals near hydraulically fractured wells explained with linear superposition method (LSM). Energies 14. https://doi.org/10.3390/en14113256.
Widdicombe, S., Blackford, J.C., Spicer, J.I., 2013. Assessing the environmental consequences of CO2 leakage from geological CCS: generating evidence to support environmental risk assessment. Mar. Pollut. Bull. 73, 399–401. https://doi.org/10.1016/j.marpolbul.2013.05.044.
Wu, K., Olson, J.E., 2015. A simplified three-dimensional displacement discontinuity method for multiple fracture simulations. Int. J. Fract. 193 (2), 191–204. https://doi.org/10.1007/s10704-015-0023-4.
Zheng, F., Jahandideh, A., Jha, B., Jafarpour, B., 2021. Geologic CO2 storage optimization under geomechanical risk using coupled-physics models. Int. J. Greenh. Gas Control 110. https://doi.org/10.1016/j.ijggc.2021.103385.
Zoback, M.D., 2007. Reservoir Geomechanics. Cambridge University Press.
Zoback, M.D., Gorelick, S.M., 2012. Earthquake triggering and large-scale geologic storage of carbon dioxide. Proc. Natl. Acad. Sci. U. S. A. 109, 10164–10168. https://doi.org/10.1073/pnas.1202473109.